

2015

Fatty Acyl Incorporation in the Biosynthesis of WAP-8294A, a Group of Potent Anti-MRSA Cyclic Lipodepsipeptides

Haotong Chen
University of Nebraska-Lincoln

Andrew S. Olson
University of Nebraska-Lincoln, aolson13@unl.edu

Wei Su
University of Nebraska-Lincoln

Patrick Dussault
University of Nebraska-Lincoln, pdussault1@unl.edu

Liangcheng Du
University of Nebraska - Lincoln, ldu3@unl.edu

Follow this and additional works at: <http://digitalcommons.unl.edu/chemistrydussault>

Chen, Haotong; Olson, Andrew S.; Su, Wei; Dussault, Patrick; and Du, Liangcheng, "Fatty Acyl Incorporation in the Biosynthesis of WAP-8294A, a Group of Potent Anti-MRSA Cyclic Lipodepsipeptides" (2015). *Patrick Dussault Publications*. 34.
<http://digitalcommons.unl.edu/chemistrydussault/34>

This Article is brought to you for free and open access by the Published Research - Department of Chemistry at DigitalCommons@University of Nebraska - Lincoln. It has been accepted for inclusion in Patrick Dussault Publications by an authorized administrator of DigitalCommons@University of Nebraska - Lincoln.



Published in final edited form as:

RSC Adv. 2015 ; 5: 105753–105759. doi:10.1039/c5ra20784c.

Fatty Acyl Incorporation in the Biosynthesis of WAP-8294A, a Group of Potent Anti-MRSA Cyclic Lipodepsipeptides

Haotong Chen^{a,†}, Andrew S. Olson^{a,†}, Wei Su^a, Patrick H. Dussault^{*,a}, and Liangcheng Du^{*,a}

^aDepartment of Chemistry, University of Nebraska-Lincoln, Lincoln, NE, 68588-0304, USA

Abstract

WAP-8294A is a family of at least 20 cyclic lipodepsipeptides exhibiting potent anti-MRSA activity. These compounds differ mainly in the hydroxylated fatty acyl chain; WAP-8294A2, the most potent member of the family that reached clinical trials, is based on (*R*)-3-hydroxy-7-methyloctanoic acid. It is unclear how the acyl group is incorporated because no acyl-CoA ligase (ACL) gene is present in the WAP-8294A gene cluster in *Lysobacter enzymogenes* OH11. Here, we identified seven putative ACL genes in the OH11 genome and showed that the yield of WAP-8294A2 was impacted by multiple ACL genes with the ACL6 gene having the most significant effect. We then investigated several (*R*)-3-hydroxy fatty acids and their acyl SNAC (*N*-acetylcysteamine) thioesters as substrates for the ACLs. Feeding (*R*)-3-hydroxy-7-methyloctanoate-SNAC to the ACL6 gene deletion mutant restored the production of WAP-8294A2. Finally, we heterologously expressed the seven ACL genes in *E. coli* and purified six of the proteins. While these enzymes exhibit a varied level of activity *in vitro*, ACL6 showed the highest catalytic efficiency in converting (*R*)-3-hydroxy-7-methyloctanoic acid to its CoA thioester when incubated with coenzyme A and ATP. These results provided both *in vivo* and *in vitro* evidence to support the fact that ACL6 is the main player for fatty acyl activation and incorporation in WAP-8294A2 biosynthesis. The results also suggest that the molecular basis for the acyl chain diversity in the WAP-8294A family is the presence of functionally overlapping ACLs.

Introduction

The discovery of new anti-infective drugs is a pressing and continual need for human health due to the constant emergence of drug resistant pathogens.^{1,2} Nosocomial infections caused by methicillin-resistant *Staphylococcus aureus* (MRSA) have become an especially serious clinical problem. It is imperative to discover and develop new antibiotics. Natural products (NPs) are the most significant source of anti-infectives³ and we have been using *Lysobacter* species as a new source for bioactive NP discovery.^{4–10} WAP-8294A (Fig. 1), a family of compounds displaying anti-MRSA activity, are cyclic lipodepsipeptides originally isolated

*Corresponding authors, ldu3@unl.edu; pdussault1@unl.edu.

†HC and ASO contribute equally.

Electronic Supplementary Information (ESI) available: [Descriptions of primer design and sequences, plasmid construction, protein expression and purification, kinetic data, organic synthesis and detailed protocols for experimental procedures]. See DOI: 10.1039/x0xx00000x

from *Lysobacter staphylocidin*.^{11–13} Cyclic depsipeptides belong to a large and diverse family of nonribosomally synthesized peptides that have a wide variety of important biological activities.^{14–16} WAP-8294A2 (lotilibicin), the most potent antibacterial of the family, exhibit 14-fold greater anti-MRSA activity compared with vancomycin; an IV formulation was in phase-I clinical studies in 2010.^{12,17,18}

Although WAP-8294A compounds were first isolated nearly two decades ago, the study of their biosynthetic mechanism was reported only in 2011.^{11,12} Improved understanding of the molecular mechanism of biosynthesis could open rational approaches to generate new analogs with improved clinical properties. We have identified the WAP biosynthetic gene cluster from *L. enzymogenes* OH11, which includes two large nonribosomal peptide synthetase (NRPS) genes. The NRPSs comprise a total of 12 modules that make 45 functional domains, which are responsible for the assembly of the 12-amino acid core structure of WAP-8294A compounds.¹¹

The WAP-8294A family all contains a 3-acyloxy amide linkage derived from a (*R*)-3-hydroxy fatty acyl chain; individual family members differ in the length of the chain and the presence or absence of a branching methyl group (Fig. 1). The fatty acids must be activated before incorporation into the peptide. The mechanism is likely to involve activation of fatty acids to their corresponding acyl coenzyme A (CoA) thioesters by a family of acyl CoA ligases (ACL). This catalytic process occurs in two steps and involves requisite formation of an acyladenylate (acyl-AMP) intermediate.¹⁹ Acyl CoA ligases are usually located within the biosynthetic cluster associated with formation of the remainder of the natural product. For example, the gene clusters for amphi-enterobactin,²⁰ daptomycin¹⁶ and calcium-dependent antibiotic (CDA)²¹ all host a dedicated ACL and an ACP (acyl carrier protein) for the activation and incorporation of the fatty acyl chain. It is therefore interesting that there is no ACL gene present in or near the WAP gene cluster,¹¹ a phenomenon previously observed with the gene cluster for surfactin.²² In addition, no dedicated ACP is present within the WAP cluster. These features suggest that the WAP-8492A biosynthetic pathway likely recruits an ACL *in trans* and that the fatty acids are directly activated as acyl-*S*-CoA thioesters, instead of acyl-*S*-ACP, for the incorporation into the peptide core.

The aim of this work is to determine the molecular basis for activation and incorporation of fatty acyl chains in the biosynthesis of members of the WAP-8294A family, particularly for the most eminent member WAP-8294A2. Here we describe both the *in vivo* and *in vitro* results obtained from the study of seven putative ACLs found in the genome of *L. enzymogenes* OH11. Our study shows that multiple ACLs contribute to WAP-8294A biosynthesis and that ACL6 is the most important enzyme in the activation of (*R*)-3-hydroxy-7-methyloctanoic acid and incorporation into WAP-8294A2.

Results and discussion

Multiple acyl-CoA ligases contribute to WAP-8294A biosynthesis

We identified seven putative ACL genes in the genome of *L. enzymogenes* OH11 that are associated with secondary metabolism (Fig. S1A). The ACL genes are either associated with NRPS-PKS gene clusters, or adjacent to genes related to biosynthesis and regulation of

natural products, such as genes encoding lantibiotic-modifying enzyme, enoyl-CoA hydratase, or two-component regulatory system. To test if any of the ACLs is involved in WAP-8294A biosynthesis, we disrupted each of the 7 ACL genes (Fig. S2 and S3). The HPLC and MS analysis showed that the disruption of ACL1, ACL5, and ACL7 had little impact on the yield of WAP-8294A2, whereas the disruption of ACL2, ACL3, ACL4, and ACL6 significantly reduced the yield (Fig. 2). In particular, the ACL6 mutant produced a barely detectable amount of WAP-8294A2. Thus we mainly focused on ACL6 in subsequent experiments. The results suggest that multiple ACLs contribute to the fatty acyl chain activation and incorporation in WAP-8294A2 biosynthesis, and the ACLs are functionally redundant.

Feeding fatty acyl precursor restored WAP-8294A2 production in ACL6 in-frame deletion mutants

To eliminate potential polar effects caused by insertion of the conjugal vector in the gene disruption mutants, we also generated in-frame deletion mutants for ACL6 gene (Fig. S3). WAP-8294A2 production in this mutant strain was monitored by HPLC and MS (Fig. 3). Similar to that in the ACL6 disruption mutant, WAP-8294A2 production in the in-frame deletion mutant was nearly completely eliminated. We chemically synthesized the *N*-acetyl cysteamine thioester (SNAC) of (*R*)-3-hydroxy-7-methyloctanoic acid (Fig. 4); details are provided in Supplementary Information. This compound was used as the acyl-CoA surrogate to be fed to the ACL6 deletion mutant. HPLC analysis clearly showed that WAP-8294A2 production was restored in the ACL6 mutant (Fig. 3). This result demonstrated that ACL6 is the predominant enzyme responsible for fatty acyl incorporation into WAP-8294A2.

Heterologous expression of ACL genes and *in vitro* assay of the enzyme activity

We cloned the seven putative ACL genes in pET28A and heterologously expressed the genes in *E. coli*. The expressed proteins were purified, except ACL2 which was produced mostly as an insoluble protein (Fig. S4). As judged by SDS-PAGE, the observed molecular masses of ACL1 through ACL7, including the His₆ tag, were consistent with the predicted masses (58.7, 58.8, 60.4, 59.8, 61.0, 47.2, 58.6 kDa) calculated from the amino acid sequences (Fig. S4).

The enzyme activity of ACLs 1–7 was measured by incubating the enzymes with (*R*)-3-hydroxy-7-methyloctanoic acid, ATP, and CoA. A distinct peak in HPLC was detected around 9.2 min in the reaction containing ACL6. This peak was collected and analyzed by MS, which gave a [M+H]⁺ of *m/z* 924.93, consistent with the mass of 3-hydroxy-7-methyloctanoyl-CoA (calculated mass 923.23) (Fig. 5 and S5). Tandem mass spectrometry was used to fragment the analytes into product ions. Both the fatty acyl-CoA precursor ion (*m/z* 924.30) and its product ions (*m/z* 428.10, 417.20) were detected, while the control reaction (w/o enzyme) only gave the product ions of CoA (*m/z* 480.10 and *m/z* 261.20). The results support the hypothesis that ACL6 catalyzes acyl-CoA formation from the fatty acid and CoA. Other ACL also showed some activity, but the product was formed in such minute amounts that the peak could only be detected by MS. In addition, we tested (*R*)-3-hydroxyoctanoic acid, which corresponds to the fatty acyl portion of WAP-8294A1 (Fig. 1).

HPLC and MS data showed a peak around 9 min that gave a $[M+H]^+$ of m/z 911.00 when ACL5 was incubated with (*R*)-3-hydroxyoctanoic acid, CoA and ATP (data not shown). The result indicates that ACL5 is able to catalyze the acyl-CoA formation from (*R*)-3-hydroxyoctanoic acid and CoA.

To further confirm the specificity of the enzymes, we performed kinetic analysis, using EnzChek Pyrophosphate Assay Kit. The inorganic pyrophosphatase in this kit catalyzes conversion of PPi into two equivalents of Pi. The Pi is then consumed by the 2-amino-6-mercapto-7-methyl-purine ribonucleoside (MESG) by purine ribonucleoside phosphorylase (PNP) and the product, 2-amino-6-mercapto-7-methyl purine, is detected by an increase in absorbance at 360 nm. The EnzChek Pyrophosphate Assay Kit had been used for the quantitation of PPi in solution or for the continuous determination of PPi released in enzymatic reactions.^{23–25} To measure the activity, ACL was incubated with free fatty acid, ATP, CoA and the coupled reaction system provided by the kit as described above. The kinetic parameters were determined by initial velocity experiments using the coupled assay (Table S2A and S2B). These data were globally fitted to Michaelis-Menten Equation, yielding K_m values for (*R*)-3-hydroxy-7-methyloctanoic acid and (*R*)-3-hydroxyoctanoic acid. The data confirmed that ACL6 favored (*R*)-3-hydroxy-7-methyloctanoic acid as substrate, while ACL5 had a faster rate when (*R*)-3-hydroxyoctanoic was the substrate. The relatively slow reaction rates might explain the very low yield of WAP-8294A in *L. enzymogenes*.¹¹ No steady signal was detected in the enzyme-free or ATP-free control reactions, showing that the detected signals resulted from the enzymatic activity of ACLs.

Conclusions

Cyclic lipopeptides are an important group of bioactive natural products; this is exemplified by the new antibiotic daptomycin (Cubicin). Although many of the peptides exhibit activity, WAP-8294A2 is exceptionally potent against MRSA (ED₅₀ 14-fold lower than vancomycin). WAP-8294A2 reached the Phase-I clinical studies, but appears to have been discontinued from the clinical development.¹⁸ The reason for discontinuation has not been published, but could indicate undesirable pharmaco-properties. The understanding of WAP-8294A biosynthetic mechanism is an essential step toward rational engineering the biosynthetic machinery to produce new analogs with improved properties. In WAP-8294A biosynthesis, the mechanism by which the 3-hydroxy fatty acyl chain is incorporated into the peptide is the least understood step.

To get more insights into the molecular basis for the fatty acyl incorporation and WAP-8294A structural diversity, we searched the genome of *L. enzymogenes* OH11 and identified seven putative ACL genes. We disrupted each of the seven ACL genes and found that none of the mutants completely lost WAP production. The result supports the notion that multiple ACL genes are involved in the acyl incorporation, and the function of the ACLs is likely redundant. Among the seven mutants, ACL6 appeared to have the highest impact on the yield of WAP-8294A2. To prove this, we generated in-frame deletion mutant of ACL6 to eliminate potential polar effects caused by gene disruption. We then chemically synthesized the acyl-CoA surrogate, (*R*)-3-hydroxy-7-methyloctanoyl SNAC. WAP-8294A2 production in the ACL6 deletion mutant was restored upon feeding the synthetic acyl-CoA

surrogate. The result confirms ACL6's role in WAP-8294A2 biosynthesis; it also suggests that ACL6 is required for substrate activation, but not NRPS priming. The results support that the WAP-8492A biosynthetic pathway recruits ACL *in trans* and that the first condensation domain in the WAP-8492A NRPS can accept acylS-CoA for the incorporation of the fatty acyl chain into the peptide core. Interestingly, a phylogenetic analysis of the condensation domains of a group of selected NRPS showed that the first C domain of WAP-8492A NRPS (WAP_WAPS1_C1) falls into the same subgroup that includes the first C domain of Calcium-Dependent Antibiotics (CDA) and Daptomycin, whose biosynthesis uses acyl-ACP as substrate (Fig. S1B).

In the *in vitro* studies, we were able to express six of the seven putative ACL genes in *E. coli* and to purify the proteins for enzyme activity assay and kinetic studies. The enzyme activity was demonstrated by the conversion of the chemically synthesized (*R*)-3-hydroxy fatty acids to the corresponding CoA thioesters, when the purified ACLs were incubated with the substrate, CoA and ATP. The kinetic data revealed that (*R*)-3-hydroxy-7-methyloctanoic acid is the preferred substrate for ACL6. These observations are consistent with the results obtained from ACL mutants and *in vivo* feeding experiment. Together, the results support that ACL6 is the most important enzyme for fatty acyl incorporation into WAP-8294A2, and ACL5 may be an important contributor for the fatty acyl incorporation into WAP-8294A1. Based on the results presented in this study, we propose a mechanism for the initiation of the biosynthesis of WAPs, as shown in Fig. 6.

Experimental procedures

Chemicals, bacterial strains, plasmids, and general procedures for DNA manipulation

Chemicals used in this study were purchased from Fisher Scientific, Sigma, and Acros. Oligonucleotide primers for PCR were synthesized by Eurofins MWG Operon. Plasmid preparation and DNA extraction were carried out with Qiagen kits (Valencia, CA), and all other DNA manipulations were carried out according to standard methods. Ni-NTA agarose was purchased from Qiagen (Valencia, CA). *Escherichia coli* strain XL Blue was used as the host for general plasmid DNA propagation, and the cloning vector was pANT841. Vector pET28a was used for protein expression in *E. coli* BL21 (DE3). *E. coli* S17-1 was used as the conjugal strain to transfer DNA into *Lysobacter*. *L. enzymogenes* and other bacterial strains were grown in Luria-Bertani (LB) broth medium, 1/10-strength tryptic soy broth (1/10 TSB, Sigma) or NYGB/A medium. EnzChek Pyrophosphate Assay Kit was purchased from Sigma.

Generation of gene disruption mutants

To construct plasmids for gene disruption, an internal fragment was amplified from each of the open reading frames (ORFs) using the primer pairs described in Supporting Information (Table S1). Genomic DNA from the wild type *L. enzymogenes* OH11 served as the PCR template. The homologous regions of these ACLs were amplified by PCR and introduced into the conjugation vector pJQ200SK to produce pJQ200SK-ACLs. Each of the pJQ200SK constructs was transformed into *E. coli* S17-1, which was mated with *L. enzymogenes* OH11 for conjugal transfer of the vectors. The positive colonies grown on LB plates containing

gentamicin (20 µg/mL) were picked up and inoculated into liquid cultures containing gentamicin. Genomic DNA was prepared from each of the cultures, and diagnostic PCR was performed to identify mutants that resulted from a homologous recombination. To screen the ACL gene disruption mutants, PCR was performed using the diagnostic primers listed in Table S1, which would amplify correct fragments when mutants resulted from a homologous recombination, but not from the wild type or mutants resulted from a random insertion of the construct (Fig. S2 and S3).

Production and analysis of metabolites in mutant strains

L. enzymogenes OH11 and its mutants were grown in 1/10 TSB for 1 day, and an aliquot of 200 l was spread on a solid NYGA plate (bacteriological peptone, 5 g/L; yeast extract, 3 g/L; glycerol, 20 g/L, and agar 15 g/L). The plates were incubated at 28 °C for 2 days. To extract the metabolites, the solid media were collected and extracted with methanol. The methanol extract was dried with a rotavapor (Buchi, Rotavapor R-200) to afford the crude extract, which was dissolved in 2 mL methanol containing 0.05% TFA. A 20 µl aliquot of each of the extracts was analyzed by HPLC (1220 Infinity LC, Agilent Technologies) using a reversed-phase column (Cosmosil 5C18-AR-II, 4.6 ID × 250 mm). Water/0.01 M TFA (solvent A) and acetonitrile/methanol = 1:1 (solvent B) were used as the mobile phases with a flow rate of 1.0 mL/min. The HPLC program was as follows: 57% B in A in the first 5 min, 57–100% B in 5–32 min, 100% B in 32–40 min, back to 57% B at 41 min, and maintained to 48 min. The metabolites were detected at 280 nm on a UV detector. LCQ-MS was used to verify the mass of the peak of WAP-8294A2 and analogs.

Generation of gene deletion mutants

To construct the ACL6 in-frame deletion vector, primer extension PCR reactions were performed to generate a 705-bp fragment from both the upstream and downstream regions of ACL6 gene. Homologous recombination at both regions would delete the entire ACL6 gene without interference with other genes. The primers used for these experiments are listed in the Table S1. The PCR amplified fragment was then cloned into the conjugal vector pJQ200SK as an *XhoI/BamHI* fragment to produce pJQ200SK-ACL-6. To conjugally transfer pJQ200SK-ACL-6 into *L. enzymogenes* OH11, the procedure was identical to the previously described.¹¹ The correct single crossover mutant was selected by diagnostic PCR (Fig. S3). Individual colonies of confirmed single crossover mutants were subjected to liquid cultures containing 5% (W/V) sucrose to select for the loss of the vector through a second homologous recombination. The single crossover mutants were grown in 1/10 TSB medium for 14 hours. Then the individual cultures were re-inoculated into 1/10 TSB (with 1:100 ratio) containing 5% sucrose and 25 µg/mL kanamycin medium. Aliquots (50 µl) were removed every 3 hours from this liquid culture and spread onto 1/10 TSA plates (5% sucrose, 25 µg/mL kanamycin). Single colonies were picked up from the plates and allowed to grow in 1/10 TSB (5% sucrose, 25 µg/mL kanamycin) liquid medium for another 2–5 days. To confirm the double crossover mutant, another diagnostic PCR was performed using genomic DNA extracted from the single colonies as template (Fig. S3).

Synthesis of (*R*)-3-hydroxy fatty acids and (*R*)-3-hydroxy fatty acyl SNAC

To generate the initial carbon backbone, we generated the dianion of methyl acetoacetate with LDA then subsequent alkylation with an appropriate bromoalkane to create the target carbon skeleton in roughly 20–50% yields (**1a–b**) (Fig. 4).²⁶ A subsequent asymmetric reduction of the β -keto ester with borane dimethyl sulfide complex in the presence of a commercial oxazaborolidine catalyst provides the beta hydroxy esters **2a–b** in 20–40% yield with a 90–92% enantiomeric excess of the *R* isomer.²⁷ Hydrolysis of the methyl esters to the carboxylic acids can be accomplished in almost quantitative yield (**3a–b**) in the presence of LiOH. Selective formation of thioesters **4a–b** in the presence of the free alcohol is accomplished in 70–80% yield through carbodiimide-mediated coupling with SNAC in the presence of stoichiometric DCC and catalytic DMAP (see Supporting Information for details).

Feeding of ACL6 deletion mutant with 3-hydroxy-7-methyloctanoyl SNAC

ACL6 in-frame deletion mutant was grown in 1/10 TSB for 1 day, and an aliquot of 1 mL was inoculated into two 1 liter NYGB liquid cultures. The culture was fed with the fatty acyl-SNAC dissolved in DMSO under pulse feeding on 2 following days (0.12 mmol/L and 0.06 mmol/L) following a reported procedure.²⁸ Metabolites were extracted from the supernatant with ethyl acetate: methanol: acetic acid = 80: 15: 5. The organic phase was dried under reduced pressure (rotary evaporator) to afford the crude extract. The extract was dissolved in 2 mL methanol containing 0.05% TFA. A 20 μ L aliquot of each of the extracts was analyzed by HPLC as described above.

Expression of seven ACL genes and purification of the enzymes

To construct expression vectors, the coding region of each of the seven ACL genes was amplified by PCR using genomic DNA of *L. enzymogenes* OH11 as template. The primers are listed in Table S1. Each of the PCR fragments was digested and cloned into pANT841. The cloned gene in each of the constructs was sequenced, and the result showed that all the ACL sequences were correct. The ACL genes were released from pANT841 and cloned into the expression vector pET28a. The pET28a constructs were introduced into *E. coli* BL21(DE3). Individual colonies were inoculated in 3 mL of liquid LB medium containing kanamycin (50 μ g/mL) and incubated in a shaker (250 rpm) at 37 °C overnight. The culture was then added to 50 mL fresh LB medium and incubated in a shaker (250 rpm) at 37 °C until the cell density (OD₆₀₀) reached 0.6. To induce the expression of the ACL genes, IPTG (0.1 mM) was added to the cultures, and the cells were allowed to grow at the same conditions for another 3 h. To extract proteins, the cells were harvested and resuspended in 2 mL of Tris-HCl buffer (250 mM NaCl, 100 mM LiCl, 50 mM Tris, pH 7.8). The cell suspension was treated with lysozyme (1 mg/mL) and sonicated five times (3-second sonication with 2-second pause) on ice. The soluble fraction of protein extracts was loaded onto a Ni-NTA column, which was previously calibrated with Tris buffer containing 10 mM imidazole. The column was washed three times with Tris buffer containing 20 mM imidazole, and the His₆-tagged protein was eluted twice with 200 μ L of Tris buffer containing 250 mM imidazole. The eluted proteins were checked by SDS-PAGE (Fig. S4).

The fractions containing pure ACLs were collected and dialyzed against Tris buffer containing 15 % glycerol.

***In vitro* assay of acyl-CoA ligase activity**

Enzymatic reactions to generate fatty acyl-CoA were set up using the following conditions: 10 μ M ACL, 0.2 mM CoA, 10 mM ATP, 20 μ M fatty acid in DMSO, 5 mM MgCl₂, 0.2% (w/v) Triton, 200 μ M DTT, and 100 mM Tris-HCl pH 7.8. All reactions were incubated at 30 °C overnight. Samples were analyzed by HPLC (1220 Infinity LC, Agilent Technologies) using a reversed-phase column (Phenomenex, 4.6 ID \times 150 mm). Water containing 25 mM ammonium acetate and 0.5% acetic acid (solvent A) and acetonitrile containing 0.5% acetic acid (solvent B) were used as the mobile phases with a flow rate of 1.0 mL/min. The HPLC program was as follows: 10% B in A in the first 3 min, 10–90% B in 3–15 min, 90% B in 15–25 min, back to 10% B at 26 min, and maintained to 30 min.²⁹ The metabolites were detected at 260 nm on a UV detector. MS (Finnigan mat, LCQ) was used to verify the mass of the reaction products. LC-MS/MS was used to further confirm the product. An Agilent LC-1200 (Santa Clara, CA) was connected to a 2.1 \times 100 mm Symmetry ODS column from Waters (Milford, MA) and a Triple Quadrupole Mass Spectrometer model 4000 QTrap from ABSciex (Framingham, MA) operating in either single quadrupole (Q1), enhanced mass spectrum (EMS), MS/MS or multiple reaction monitoring (MRM) modes. The samples were injected onto the column and eluted with 98% mobile phase A (0.1% formic acid in water, J.T. Baker) to 60% B (0.1% formic acid in acetonitrile, Acros Organics) over 15 minutes, followed by 5 minutes of 98% B and 5 min of 98 % A, all at a flow rate of 0.25 mL/min.

Kinetic analysis of acyl-CoA ligase activity

The EnzChek Pyrophosphate Assay Kit (Molecular Probes™) was used to measure the activities of ACLs. A standard curve ($y = 0.0156x + 0.0004$, $R^2 = 0.99603$) for the pyrophosphate assay was generated using pyrophosphate standard as a source of PPi. To measure the activity of ACLs, the following reagents were combined in 0.1 mL reaction volumes: 0.4 mM ATP, 0.4 mM CoA, 0.4 mM free fatty acids in DMSO, 0.2 mM 2-amino-6-mercapto-7-methyl-purine ribonucleoside (MESG), 1 U purine nucleoside phosphorylase (PNP), 0.01 U pyrophosphatase, and various ACLs with final concentration of 15 μ M. After incubating at 22 °C for 30 minutes, the absorbance at 360 nm was measured and corrected for background absorbance. The substrates tested were chemically synthesized (*R*)-3-hydroxy-7-methyloctanoic acid (corresponding to the fatty acyl chain in WAP 8294-A2) and (*R*)-3-hydroxyoctanoic acid (corresponding to the fatty acyl chain in WAP 8294-A1). The kinetic parameters of ACLs were determined by initial velocity experiments using the coupled assay. These data were globally fitted to Michaelis-Menten Equation, yielding K_m values for the substrates.

Supplementary Material

Refer to Web version on PubMed Central for supplementary material.

Acknowledgments

We thank Dr. Javier Seravalli and Prof. James Takacs for technical assistance and Dr. Guoliang Qian for providing the *Lysobacter enzymogenes* strain OH11. This research was supported in part by the NIH (R01AI097260), NSFC (31329005), and a University of Nebraska-Lincoln Redox Biology Center pilot grant.

Notes and references

1. Walsh CT, Wencewicz TA. *J Antibiot.* 2014; 67:7. [PubMed: 23756684]
2. Cooper MA, Shlaes D. *Nature.* 2011; 472:32. [PubMed: 21475175]
3. Newman DJ, Cragg GM. *J Nat Prod.* 2012; 75:311. [PubMed: 22316239]
4. Han Y, Wang Y, Tombosa S, Wright S, Huffman J, Yuen G, Qian G, Liu F, Shen Y, Du L. *Appl Microbiol Biotechnol.* 2015; 99:801. [PubMed: 25301587]
5. Li Y, Chen H, Ding Y, Xie Y, Wang H, Cerny RL, Shen Y, Du L. *Angew Chem Int Ed Engl.* 2014; 53:7524. [PubMed: 24890524]
6. Wang Y, Qian G, Liu F, Li YZ, Shen Y, Du L. *ACS Synth Biol.* 2013; 2:670. [PubMed: 23937053]
7. Wang Y, Qian G, Li Y, Wright S, Shen Y, Liu F, Du L. *PLoS One.* 2013; 8:e66633. [PubMed: 23826105]
8. Xie Y, Wright S, Shen Y, Du L. *Nat Prod Rep.* 2012; 19:1277. [PubMed: 22898908]
9. Lou L, Chen H, Cerny RL, Li Y, Shen Y, Du L. *Biochemistry.* 2012; 51:4–6. [PubMed: 22182183]
10. Lou L, Qian G, Xie Y, Hang J, Chen H, Zaleta-Rivera K, Li Y, Shen Y, Dussault PH, Liu F, Du L. *J Am Chem Soc.* 2011; 133:643. [PubMed: 21171605]
11. Zhang W, Li Y, Qian G, Wang Y, Chen H, Li YZ, Liu F, Shen Y, Du L. *Antimicrob Agents Chemother.* 2011; 55:5581. [PubMed: 21930890]
12. Kato A, Nakaya S, Ohashi Y, Hirata H. *J Am Chem Soc.* 1997; 119:6680.
13. Kato A, Hirata H, Ohashi Y, Fujii K, Mori K, Harada K. *J Antibiot.* 2011; 64:373. [PubMed: 21326252]
14. Baltz RH, Miao V, Wrigley SK. *Nat Prod Rep.* 2005; 22:717. [PubMed: 16311632]
15. Baltz RH. *Nat Biotechnol.* 2006; 24:1533. [PubMed: 17160059]
16. Baltz RH. *Curr Top Med Chem.* 2008; 8:618. [PubMed: 18473888]
17. Pirri G, Giuliani A, Nicoletto SF, Pizzuto L, Rinaldi AC. *Central Eur J Biol.* 2009; 4:258.
18. Butler MS, Blaskovich MA, Cooper MA. *J Antibiot.* 2013; 66:571. [PubMed: 24002361]
19. Arora P, Goyal A, Natarajan VT, Rajakumara E, Verma P, Gupta R, Yousuf M, Trivedi OA, Mohanty D, Tyagi A, Sankaranarayanan R, Gokhale RS. *Nat Chem Biol.* 2009; 5:166. [PubMed: 19182784]
20. Zane HK, Naka H, Rosconi F, Sandy M, Haygood MG, Butler A. *J Am Chem Soc.* 2014; 136:5615. [PubMed: 24701966]
21. Chong PP, Podmore SM, Kieser HM, Redenbach M, Turgay K, Marahiel M, Hopwood DA, Smith CP. *Microbiol.* 1998; 144:193.
22. Kraas FI, Helmetag V, Wittmann M, Strieker M, Marahiel MA. *Chem Biol.* 2010; 17:872. [PubMed: 20797616]
23. Chhabra ES, Higgs HN. *J Biol Chem.* 2006; 281:26754. [PubMed: 16818491]
24. Lee YH, Gallant C, Guo H, Li Y, Wang CA, Morgan KG. *J Biol Chem.* 2000; 275:3213. [PubMed: 10652307]
25. Vergnolle O, Xu H, Blanchard JS. *J Biol Chem.* 2013; 288:28116. [PubMed: 23935107]
26. Huckin SN, Weiler LS. *J Am Chem Soc.* 1974; 96:1082.
27. Hasdemir B, Onar HC, Yusufoglu A. *Tetrahedron-Asymmetry.* 2012; 23:1100.
28. Werneburg M, Busch B, He J, Richter MEA, Xiang LK, Moore BS, Roth M, Dahse HM, Hertweck C. *J Am Chem Soc.* 2010; 132:10407. [PubMed: 20662518]
29. Dalluge JJ, Gort S, Hobson R, Selifonova O, Amore F, Gokarn R. *Analyt Bioanal Chem.* 2002; 374:835.

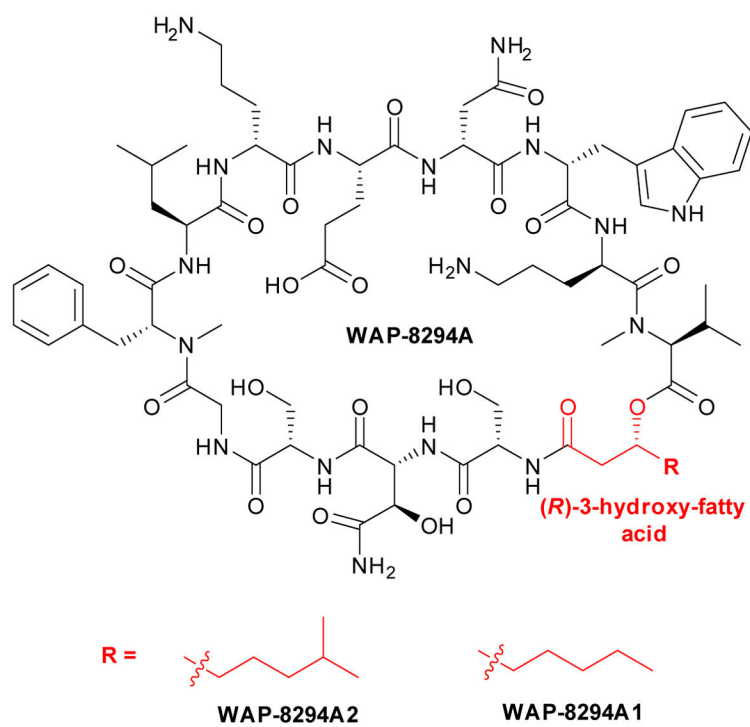


Fig. 1.
Structure of the two main members of the WAP-8294A family.

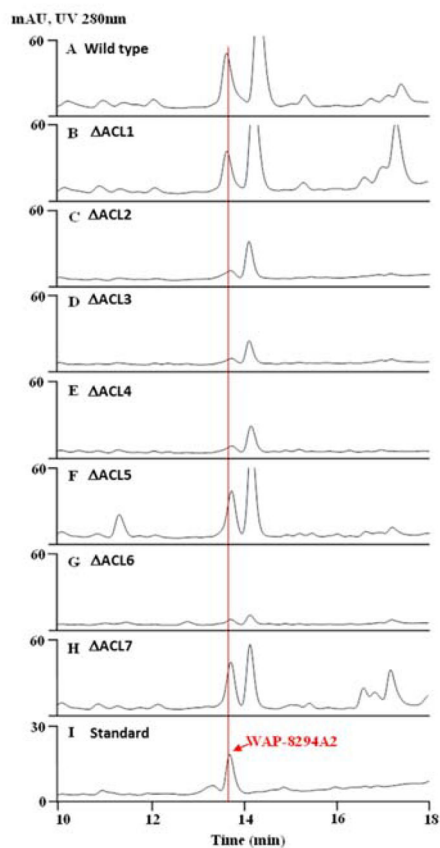


Fig. 2. HPLC analysis of metabolites from various strains of *Lysobacter enzymogenes* OH11. A: OH11 wild type; B-H: disruption mutants of ACL1 through ACL7, respectively; I: WAP-8294A2 standard. The detection wavelength was 280 nm.

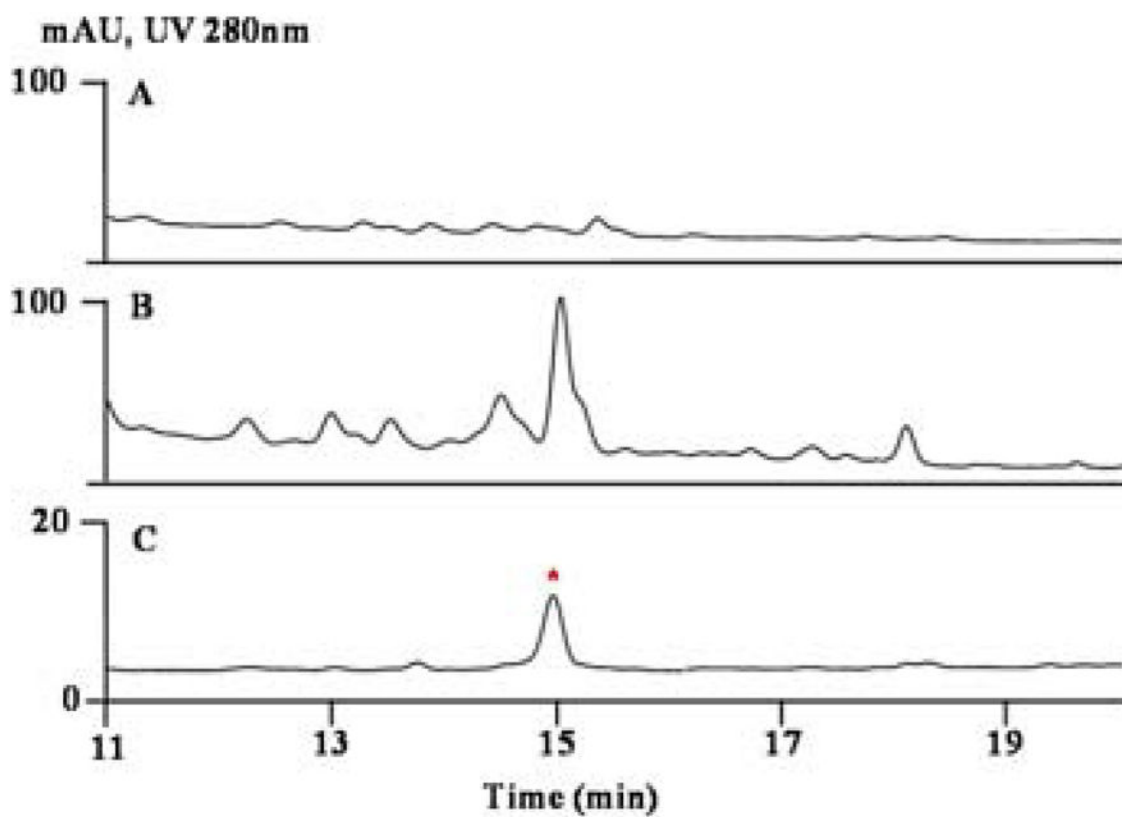


Fig. 3. HPLC analysis of metabolites in strains of *Lysobacter enzymogenes* OH11. A: ACL6 in-frame deletion mutant; B: The ACL6 mutant supplemented with (*R*)-3-hydroxy-7-methyloctanoic acyl-SNAC; C: WAP-8294A2 standard.

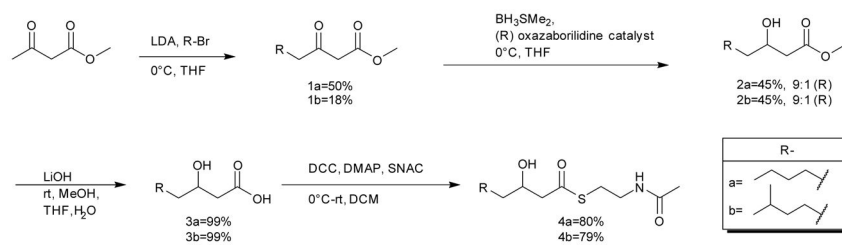


Fig. 4. Chemical synthesis of (*R*)-3-hydroxy fatty acids and 3-hydroxy fatty acyl-SNAC (acyl thioester of *N*-acetyl cysteamine).

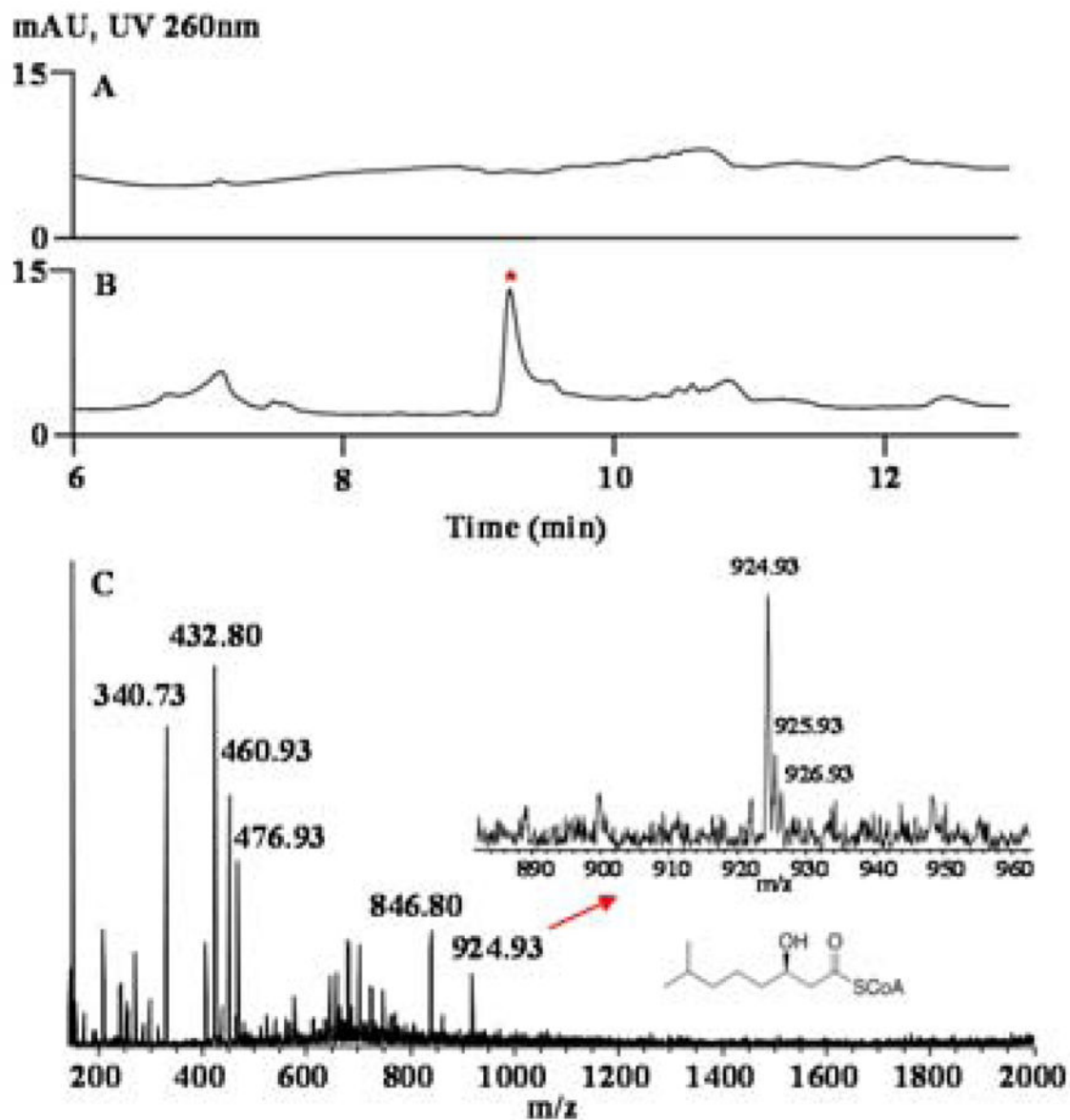


Fig. 5. HPLC and MS analysis of *in vitro* reaction products of ACL6 incubated with 3-hydroxy-7-methyloctanoic acid, ATP, and CoA. The ESI-MS signals were measured in positive single ion mode. A: HPLC of control reaction (without enzyme); B: HPLC of ACL6 reaction; C: ESI-MS analysis of the ACL6 reaction product, the distinct peak in HPLC as indicated by a star. The calculated mass of 3-hydroxy-7-methyloctanoyl-CoA is 923.23 (see Fig. S5).

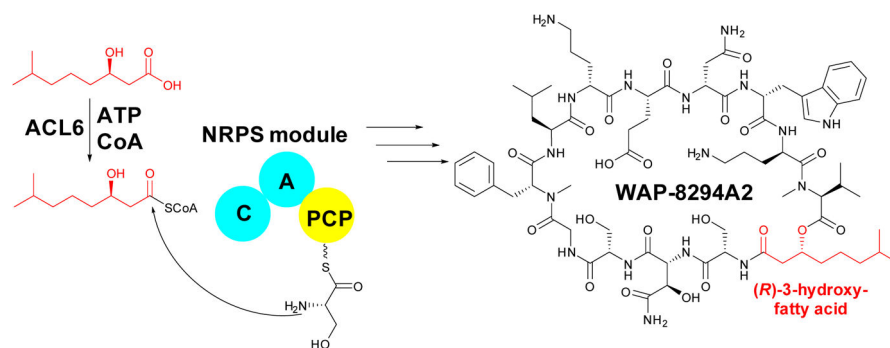


Fig. 6. Proposed mechanism for fatty acid incorporation in WAP-8294A2 biosynthesis. The fatty acid, *(R)*-3-hydroxy-7-methyloctanoic acid, is activated by ACL6, and the resultant acyl-CoA is then recognized by the condensation (C) domain of the NRPS, which catalyzes the amide bond formation between the PCP-bound L-serine and the fatty acyl-CoA.